Int. J. Heat Mass Transfer. Vol. 15, pp. 2187–2201. Pergamon Press 1972. Printed in Great Britain

LOW PÉCLÉT NUMBER MASS TRANSFER IN LAMINAR FLOW THROUGH CIRCULAR TUBES

C. W. TAN
The Cooper Union for the Advancement of Science and Art, New York, New York, U.S.A.

and

CHIA-JUNG HSU
Brookhaven National Laboratory, Upton, New York, U.S.A.

(*Received* 25 *March* 1971 *and in revised form* 10 *January* 1972)

Abstract—Entrance-region mass transfer of diffusing matters in laminar flow through a circular tube is studied for two cases of diffusion, with and without particle formation in flight within the tube. To allow for the effects of axial diffusion, which is significant at low diffusion Péclét numbers, Pe, the domain of diffusion is extended into the region upstream of the tube ($z < 0$) besides that occupied by the tube ($z > 0$), and a uniform concentration is prescribed at $z = -\infty$. The eigenvalues are computed for the two regions and the first twenty of them are obtained for $Pe = 1{\cdot}5$, 3, 5, 10, 20, 30, 45 and ∞. By constructing two sets of orthonormal functions from the non-orthogonal eigenfunctions, the series expansion coefficients are then determined by matching both the concentrations and the longitudinal concentration gradients of the two regions at $z = 0$. The concentration solutions corresponding to $Pe = \infty$ are in excellent agreement with our previous semi-infinite region ($z > 0$) analysis. The effects of axial diffusion on the concentration distributions, the fraction of diffusing matters penetrating the tube, and the local Sherwood number are presented for various Péclét numbers and particle-generation parameter, Q.

NOMENCLATURE

A_n, coefficients of series expansion in equation (10);
B_n, coefficients of series expansion in equation (11);
c, mass concentration of diffusing matters, with subscript 1 denoting that in $z < 0$ region, and 2 in $z > 0$ region;
c_b, local bulk concentration in the $z > 0$ region, defined as $\int_0^{r_0} uc_2 r\mathrm{d}r / \int_0^{r_0} ur\mathrm{d}r$;
c_j, fully established mass concentration given by equation (4);
c_0, uniform concentration at $z = -\infty$;
D, coefficient of diffusion;
$[E]$, matrix defined below equation (21);
$[F]$; matrix defined below equation (21);
$F^*(\mu)$; fraction of diffusing matters arriving at μ, defined by equation (25);
$[G]$, matrix defined below equation (21);
Pe, diffusion Péclét number, defined as $2\bar{u}r_0/D$;
p_n^k, constant coefficients of series expansion in equation (17);
Q, nondimensional generation parameter, defined as qr_0^2/Dc_0;
q, rate of generation of diffusing matters per unit volume of gas;

q_n^k, constant coefficients of series expansion in equation (17);
r, radial coordinate distance, $0 \leqslant r \leqslant r_0$;
r_0, inner radius of tube;
$Sh(\mu)$, local Sherwood number, defined as $h_D(2r_0)/D$ where h_D is the mass-transfer coefficient;
u, axial flow velocity;
$\bar{u}$, mean flow velocity;
$X_n(\eta)$, $Y_n(\eta)$, eigenfunctions given by equations (10) and (11), respectively;
$\tilde{X}_n(\eta)$, $\tilde{Y}_n(\eta)$, orthonormal eigenfunctions of $X_n(\eta)$ and $Y_n(\eta)$ given by equation (17);
z, axial coordinate distance, $-\infty < z < +\infty$;
α_n, eigenvalues of equations (12) and (13);
β_n, eigenvalues of equations (14) and (15);
Δ_n, $n = 1, 2, \ldots$, Gram-determinant appearing in equation (19);
δ_{ij}, Kronecker delta;
η, defined as r/r_0;
ϕ, nondimensional mass concentration, defined as c/c_0;
ϕ_b, nondimensional bulk concentration, or the fraction of diffusing matters remaining at any cross-section at distance x from the tube entrance, defined as c_b/c_0;
κ, parameter in equation (5), assumed to be unity;
μ, nondimensional axial distance, defined as $2z/r_0Pe$.

INTRODUCTION

THE PROBLEM of entrance-region mass transfer (or heat transfer) with axial diffusion (or conduction) in laminar flow through circular tubes has been widely studied as can be seen in [1–4] and the references cited therein. The effects of axial diffusion are virtually negligible in comparison with radial diffusion if the diffusion Péclét number, $Pe > 100$. For $Pe < 100$, however, axial diffusion becomes increasingly significant as Pe is reduced, and ultimately attains an order of magnitude equal to that of radial diffusion as $Pe \to 1$.

In most mass (or heat) transfer studies, it is customarily assumed that particle concentration (or temperature) is uniformly distributed at the tube inlet. This assumption becomes less realistic and virtually impossible to impose as the diffusion Péclét number becomes very small. This stems from the fact that, at low Péclét numbers, axial diffusion penetrates into regions upstream of the tube inlet enlarging, therefore, the domain of mass transfer beyond the physical displacement of the tube. It is thus necessary in treating low Péclét number diffusion in a circular tube to include mass transfer in the region upstream of the tube inlet. As such, one needs to consider mass transfer in the infinite region $-\infty < z < +\infty$, where $z = 0$ is located at the tube inlet and $z > 0$ measured along the tube in the flow direction, rather than the semi-infinite region $0 \leqslant z < \infty$ which has usually been assumed. With the domain of mass transfer extended into the $z < 0$ region, it is then realistic to impose the uniform concentration profile at $z = -\infty$.

It is the purpose of this paper to re-investigate the entrance-region mass transfer problem studied in [2, 3] only in the $z > 0$ region of a circular tube and to extend it to the infinite region $-\infty < z < +\infty$. In those studies, two cases were analyzed. The first case was where all particles enter the channel uniformly and none form within it; and the second, where no particles enter the channel, and "formation in flight" occurs within the channel. For the present study, the same two cases of diffusion, with and without information in flight in the $z > 0$ region, are again investigated only that, to allow for the effect of axial diffusion which is significant at low Péclét numbers, the concentration profile is taken to be uniform at $z = -\infty$.

A mathematical scheme for solving this type of convective mass (or heat) transfer problem in the infinite region was recently devised by Hsu [5, 6] in his study of low Péclét number entrance-region heat transfer problem, subject to a step jump in wall heat flux at $z = 0$. His general scheme of analysis will be employed in the present study. The method consists essentially of determining the eigenvalues and eigenfunctions for the regions $z \leqslant 0$ and $z \geqslant 0$ separately, and then matching both the concentrations and longitudinal concentration gradients at $z = 0$. By constructing two sets of orthonormal functions from the non-orthogonal eigenfunctions with the Gram–Schmidt orthonormalization procedure, the series expansion coefficients can then be determined so that the matching conditions at $z = 0$ are satisfied.

THEORETICAL ANALYSIS

Consider diffusion in a circular tube with cylindrical coordinates r, θ, z. The tube axis extends into the $z \geqslant 0$ region with tube inlet located at $z = 0$. Denoting the concentration in the region $z < 0$ by c_1 and in the region $z > 0$ by c_2, the steady-state diffusion equation in laminar flow through the tube of radius r_0, assuming azimuthal symmetry and constant diffusion coefficient D, is

$$u\frac{\partial c_i}{\partial z} = D\left[\frac{\partial^2 c_i}{\partial r^2} + \frac{1}{r}\frac{\partial c_i}{\partial r} + \frac{\partial^2 c_i}{\partial z^2}\right] + q\delta_{i2}, (i = 1, 2) \qquad (1)$$

where u is the axial flow velocity taken to be the Poiseuille velocity $2\bar{u}(1 - r^2/r_0^2)$ with mean velocity $\bar{u}$, q is the rate of formation of the diffusing matters per unit volume of the flowing gas, and δ_{i2} $(i = 1, 2)$ is the Kronecker delta defined as

$$\delta_{i2} = \begin{cases} 0 \text{ if } i = 1 \\ 1 \text{ if } i = 2. \end{cases}$$

For the usual first case of no formation in flight, the q-term in equation (1) can, of course, be omitted. It should be retained, however, for the second case where formation in flight or particle generation occurs in the tube in $z > 0$ region.

For the flow of a gas in which the diffusing matters are annihilated or adhere to the walls as they come into contact with the tube walls, for example, through radioactive decay into other daughter elements, the pertinent boundary conditions to be satisfied in the various regions of the infinite region are:

For the $z < 0$ region,

$$\left.\begin{aligned} c_1 &= c_0 && \text{at } z = -\infty \\ \frac{\partial c_1}{\partial r} &= 0 && \text{at } r = 0 \text{ and } r = r_0. \end{aligned}\right\} \qquad (2)$$

For the $z > 0$ region,

$$\left.\begin{aligned} c_2 &= c_f && \text{at } z = +\infty \\ \frac{\partial c_2}{\partial r} &= 0 && \text{at } r = 0 \\ c_2 &= 0 && \text{at } r = r_0 \end{aligned}\right\} \qquad (3)$$

where c_f is the fully-established concentration profile given by [2, 7]*:

$$c_f = \frac{qr_0^2}{4D}\left(1 - \frac{r^2}{r_0^2}\right). \qquad (4)$$

For the case of no formation in flight, $q = 0$ and the particle concentration at $z = +\infty$ vanishes.

Further, at the interface of the two semi-

* It is hereby asserted that the fully-established concentration assumes the same form as that in the analysis for the semi-infinite region. This assumption is valid at $Pe = \infty$, a good approximation at $1 \ll Pe < 100$, but less descriptive of the real physical picture as "back" diffusion becomes significant at $Pe \leqslant 1$.

infinite regions, the following matching conditions must also be satisfied:

$$\left.\begin{aligned} c_1 &= \kappa c_2 \\ \frac{\partial c_1}{\partial z} &= \frac{\partial c_2}{\partial z} \end{aligned}\right\} \text{at } z = 0. \qquad (5)$$

The parameter κ is the ratio of the uniform concentration in region $z < 0$ to that in $z > 0$ when equilibrium is attained. In the present situation, however, the fluids in the two semi-infinite regions are one of the same fluid and, as such, $\kappa = 1$ will be assumed. The second matching condition expresses the fact that there is no accumulation of the diffusing matters at $z = 0$.

Except for the symmetry condition at $r = 0$, the boundary conditions at $r = r_0$ for the two semi-infinite regions are not the same. It has been tacitly assumed that the tube, physically occupying the $z > 0$ region, annihilates the particles as they come into contact with the tube walls, while the $z < 0$ region is included only to account for possible back diffusion near the tube entrance. That is, the $z < 0$ region is included in the analysis so that the concentration profile at $z = 0$ can be properly adjusted when the effects of axial diffusion are significant. It has further been assumed that, for the case of formation in flight, generation of diffusing matters occurs only in the tube, $z > 0$ region, but not in regions upstream of it.

As formulated, equations (1)–(5) yield results of $Pe = \infty$ identical to those obtained by the semi-infinite region analysis at the corresponding Péclét number. At $Pe = \infty$, the formulation gives a uniform concentration profile at $z = 0$ which, in the semi-infinite region analysis, was used as an *a priori* assumption for all diffusion Péclét numbers.

For the solution of the above equations, it is convenient to introduce the following dimensionless quantities:

$$\phi = \frac{c}{c_0}, \eta = \frac{r}{r_0}, \mu = \frac{2(z/r_0)}{Pe}$$

$$Pe = \frac{2\bar{u}r_0}{D}, Q = \frac{qr_0^2}{Dc_0}.$$

Equations (1)–(5), in dimensionless form, become

$$2(1-\eta^2)\frac{\partial \phi_i}{\partial \mu} = \frac{\partial^2 \phi_i}{\partial \eta^2} + \frac{1}{\eta}\frac{\partial \phi_i}{\partial \eta} + \left(\frac{2}{Pe}\right)^2 \frac{\partial^2 \phi_i}{\partial \mu^2} + Q\delta_{i2}, (i = 1, 2) \qquad (6)$$

$$\left.\begin{aligned} \phi_1 &= 1 && \text{at } \mu = -\infty \\ \frac{\partial \phi_1}{\partial \eta} &= 0 && \text{at } \eta = 0 \text{ and } \eta = 1 \end{aligned}\right\} \qquad (7)$$

$$\left.\begin{aligned} \phi_2 &= \frac{Q}{4}(1-\eta^2) && \text{at } \mu = +\infty \\ \frac{\partial \phi_2}{\partial \eta} &= 0 && \text{at } \eta = 0 \\ \phi_2 &= 0 && \text{at } \eta = 1 \end{aligned}\right\} \qquad (8)$$

and

$$\left.\begin{aligned} \phi_1 &= \phi_2 \\ \frac{\partial \phi_1}{\partial \mu} &= \frac{\partial \phi_2}{\partial \mu} \end{aligned}\right\} \text{at } \mu = 0 \qquad (9)$$

where subscript $i = 1$ refers to the $z < 0$ region and $i = 2$, the $z > 0$ region.

The concentration distributions in the two regions are now sought in the form:

$$\phi_1 = 1 + \sum_{n=1}^{\infty} A_n X_n(\eta) \exp(\alpha_n^2 \mu), \ (\mu < 0) \qquad (10)$$

$$\phi_2 = \frac{Q}{4}(1-\eta^2) + \sum_{n=1}^{\infty} B_n Y_n(\eta) \exp(-\beta_n^2 \mu), \ (\mu > 0) \qquad (11)$$

which satisfy the conditions at $\mu = \pm\infty$. The assumed solutions include the problem of diffusion without formation in flight as a special case.

In equation (10), α_n and $X_n(\eta)$ are the eigenvalues and eigenfunctions of the following characteristic equation and boundary conditions:

$$\frac{d^2X_n}{d\eta^2} + \frac{1}{\eta}\frac{dX_n}{d\eta} + \alpha_n^2\left[\left(\frac{2}{Pe}\right)^2 \alpha_n^2 - 2(1-\eta^2)\right]X_n = 0 \quad (12)$$

$$\frac{dX_n}{d\eta} = 0 \text{ at } \eta = 0 \text{ and } \eta = 1. \quad (13)$$

Similarly, β_n and $Y_n(\eta)$ in equation (11) represent the eigenvalues and eigenfunctions for the following characteristic equation and boundary conditions:

$$\frac{d^2Y_n}{d\eta^2} + \frac{1}{\eta}\frac{dY_n}{d\eta} + \beta_n^2\left[\left(\frac{2}{Pe}\right)^2 \beta_n^2 + 2(1-\eta^2)\right]Y_n = 0 \quad (14)$$

$$\left.\begin{aligned} \frac{dY_n}{d\eta} &= 0 \quad \text{at } \eta = 0 \\ Y_n &= 0 \quad \text{at } \eta = 1. \end{aligned}\right\} \quad (15)$$

Because of the different boundary conditions imposed on both characteristic equations, the eigenvalues as well as the eigenfunctions in both regions are not equivalent. It is noted that the two sets of characteristic equations are independent of Q and, as such, the eigenvalues and their corresponding eigenfunctions thus obtained are valid for both cases of diffusion, with and without formation in flight.

Equations (12)–(15) are solved numerically with the aid of a CDC–6600 computer using the Runge–Kutta scheme. For each preassigned value of Pe, the first twenty eigenvalues and their corresponding eigenfunctions are determined. Only the first ten α's and β's and the corresponding $Y_n'(1)$ and $\int_0^1 \eta Y_n d\eta$ are tabulated in Table 1 for $Pe = 1{\cdot}5$, 3, 5, 10, 20, 30, 45 and ∞. The eigenvalues are seen to increase with increasing Péclét numbers; and at small Pe, the consecutive higher eigenvalues do not vary appreciably with magnitude. This means that in the series summation, as in equations (10) and (11), the series converges slowly at small Péclét numbers, necessitating an increase in the number of eigenvalues to be included in the computation of ϕ_1 and ϕ_2. At $Pe = \infty$, the α's are infinitely large so that $\phi_1 = 1$ in the $\mu \leqslant 0$ region giving rise to a uniform concentration at the tube inlet.

The series expansion coefficients, A_n and B_n, are contingent upon the matching of the two regions at $\mu = 0$. Substitution of equations (10) and (11) into (9) yields

$$\sum_{n=1}^{\infty} (A_n X_n - B_n Y_n) = -1 + \frac{Q}{4}(1-\eta^2)$$
$$\sum_{n=1}^{\infty} (\alpha_n^2 A_n X_n + \beta_n^2 B_n Y_n) = 0. \quad (16)$$

A_n and B_n are to be determined from the above set of coupled equations. Note that while α_n, β_n, X_n and Y_n are independent of Q, the coefficients A_n and B_n are dependent on Q. However, neither $X_n(\eta)$ nor $Y_n(\eta)$ constitutes a set of mutually orthogonal functions and, as such, the eigenfunction expansion technique commonly used for the Sturm–Liouville system cannot be utilized to evaluate the series expansion coefficients. Following Hsu [5, 6], the eigenfunctions X_n and Y_n are expanded in two complete sets of trial orthonormal functions $\tilde{X}_n$ and $\tilde{Y}_n$ such that

$$X_k = \sum_{n=1}^{k} p_n^k \tilde{X}_n(\eta)$$
$$Y_k = \sum_{n=1}^{k} q_n^k \tilde{Y}_n(\eta) \quad (17)$$

having the properties

$$\int_0^1 \tilde{Z}_i \tilde{Z}_j \, d\eta = \begin{cases} 0 \text{ if } i \neq j \\ 1 \text{ if } i = j \end{cases} \quad (18)$$

where $\tilde{Z}_n$ denotes either $\tilde{X}_n$ or $\tilde{Y}_n$. In equation (17), p_n^k and q_n^k are constant coefficients. The functions $\tilde{X}_n$ and $\tilde{Y}_n$ are complete sets for $k \to \infty$. Therefore, equation (17) is exact for $k \to \infty$. However, in practice, a finite expansion must be taken. The convergence of the method is tested by comparing results for successive k.

The two sets of orthonormal functions, $\tilde{X}_n$ and $\tilde{Y}_n$, can be constructed by the Gram–Schmidt orthonormalization procedure [5, 6],

Table 1. Eigenvalues and related constants

Pe	n	α_n	β_n	$Y_n'(1)$	$\int_0^1 \eta Y_n d\eta$	$Q = 0$: A_n	$Q = 0$: B_n	$Q = 1$: A_n	$Q = 1$: B_n
1·5	1	0·74568	1·18959	−1·15119	2·08084(1)*	−7·82070(1)*	3·67178(1)*	−7·17644(1)*	2·30007(1)*
	2	1·81309	1·94218	1·79783	−6·72013(2)	1·01316(1)	−1·32068(1)	1·71741(1)	−1·33396(1)
	3	2·37785	2·47444	−2·28297	3·37807(2)	−5·90429(2)	8·30374(2)	−8·82478(2)	9·31179(2)
	4	2·83137	2·91123	2·68393	−2·09105(2)	4·00863(2)	−6·15596(2)	5·76509(2)	−7·20282(2)
	5	3·22125	3·29073	−3·03295	1·45139(2)	−2·90988(2)	4·98359(2)	−4·10745(2)	5·96640(2)
	6	3·56860	3·63088	3·34600	−1·08154(2)	2·21839(2)	−4·20841(2)	3·09623(2)	−5·10859(2)
	7	3·88493	3·94184	−3·63230	8·45613(3)	−1·70625(2)	3·70352(2)	−2·36919(2)	4·53883(2)
	8	4·17732	4·23004	3·89769	−6·84436(3)	1·34545(2)	−3·29958(2)	1·86213(2)	−4·07047(2)
	9	4·45052	4·49985	−4·14616	5·68629(3)	−1·03603(2)	3·03064(2)	−1·43662(2)	3·75780(2)
	10	4·70787	4·75439	4·38059	−4·82137(3)	8·09550(3)	−2·77721(2)	1·12551(2)	−3·45641(2)
3	1	1·46731	1·49904	−1·09805	2·03751(1)	−5·71167(1)	6·61871(1)	−5·33437(1)	4·78404(1)
	2	2·75085	2·62331	1·72743	−7·11661(2)	1·43817(1)	−2·28055(1)	1·96745(1)	−2·18324(1)
	3	3·48798	3·39993	−2·22062	3·60181(2)	−9·32895(2)	1·42078(1)	−1·14496(1)	1·45901(1)
	4	4·10537	4·03116	2·62885	−2·20989(2)	6·46454(2)	−1·04978(1)	7·76032(2)	−1·10926(1)
	5	4·64282	4·57694	−2·98331	1·52035(2)	−4·72782(2)	8·48584(2)	−5·60894(2)	9·10373(2)
	6	5·12466	5·06466	3·30052	−1·12507(2)	3·61052(2)	−7·15469(2)	4·26033(2)	−7·74506(2)
	7	5·56513	5·50961	−3·59010	8·74981(3)	−2·77149(2)	6·29306(2)	−3·26169(2)	6·85436(2)
	8	5·97331	5·92437	3·85816	−7·05285(3)	2·18074(2)	−5·59901(2)	2·56234(2)	−6·12399(2)
	9	6·35537	6·30639	−4·10886	5·84036(3)	−1·66512(2)	5·14210(2)	−1·96026(2)	5·64245(2)
	10	6·71578	6·66929	4·34518	−4·93892(3)	1·29064(2)	−4·70452(2)	1·52296(2)	−5·17439(2)
5	1	2·36633	1·68666	−1·06160	2·00744(1)	−3·48110(1)	9·31098(1)	−3·31157(1)	7·08422(1)
	2	3·90222	3·18971	1·64959	−7·47508(2)	1·39674(1)	−3·20690(1)	1·75630(1)	−3·01542(1)
	3	4·73109	4·22604	−2·14383	3·86624(2)	−1·12154(1)	1·97444(1)	−1·26101(1)	1·96248(1)
	4	5·48110	5·06140	2·55876	−2·36395(2)	8·10501(2)	−1·45185(1)	9·01774(2)	−1·47637(1)
	5	6·14863	5·780[illegible]7	−2·91928	1·61276(2)	−6·00031(2)	1·17079(1)	−6·63241(2)	1·20486(1)
	6	6·75327	6·42041	3·24143	−1·18410(2)	4·61322(2)	−9·84867(2)	5·07914(2)	−1·02057(1)
	7	7·30929	7·00318	−3·53503	9·14952(3)	−3·53295(2)	8·65376(2)	−3·88485(2)	9·00943(2)
	8	7·82655	7·54154	3·80641	−7·33685(3)	2·77028(2)	−7·68445(2)	3·04421(2)	−8·02533(2)
	9	8·31207	8·04426	−4·05991	6·05012(3)	−2·08664(2)	7·05441(2)	−2·29800(2)	7·38506(2)
	10	8·77098	8·51758	4·29862	−5·09881(3)	1·59390(2)	−6·44020(2)	1·75983(2)	−6·75362(2)
10	1	4·31076	1·83630	−1·03061	1·98165(1)*	−8·40505(2)*	1·23853	−8·17983(2)*	9·75979(1)*
	2	6·72818	3·92223	1·52178	−7·91845(2)	6·46072(2)	−4·70985(1)*	7·56236(2)	−4·39316(1)
	3	7·58890	5·45451	−1·98549	4·35690(2)	−9·11396(2)	2·85308(1)	−9·39775(2)	2·77910(1)
	4	8·43978	6·68867	2·40159	−2·70883(2)	8·27504(2)	−2·07654(1)	8·74172(2)	−2·06121(1)
	5	9·27422	7·74508	−2·77052	1·83801(2)	−6·48664(2)	1·66496(1)	−6·82251(2)	1·66913(1)
	6	10·05903	8·68188	3·10165	−1·33350(2)	5·09510(2)	−1·39386(1)	5·35104(2)	−1·40525(1)
	7	10·79544	9·53149	−3·40335	1·01775(2)	−3·87837(2)	1·22104(1)	−4·07440(2)	1·23557(1)
	8	11·48920	10·31402	3·68181	−8·07189(3)	2·99431(2)	−1·08005(1)	3·14769(2)	−1·09554(1)

	9	12·14600	11·04294	−3·94145	6·59406(3)	−2·14302(2)	9·89597(2)	−2·26097(2)	1·00560(1)
	10	12·77069	11·72779	4·18553	−5·51338(3)	1·52713(2)	−8·99707(2)	1·61888(2)	−9·15416(2)
20	1	7·53006	1·89122	−1·01885	1·97180(1)	−4·75702(3)	1·39548	−4·68895(3)	1·11586
	2	11·74398	4·41861	1·41845	−8·17136(2)	3·23769(3)	−6·29666(1)	3·53307(3)	−5·87852(1)
	3	13·29427	6·54521	−1·79323	4·84176(2)	−1·34726(2)	3·90758(1)	−1·30900(2)	3·77826(1)
	4	14·18306	8·33580	2·16730	−3·18484(2)	3·13038(2)	−2·83489(1)	3·35229(2)	−2·78571(1)
	5	14·94893	9·88705	−2·52486	2·21739(2)	−3·90920(2)	2·25916(1)	−3·98946(2)	2·24011(1)
	6	15·80082	11·26633	2·85809	−1·61521(2)	3·43097(2)	−1·88689(1)	3·53901(2)	−1·88096(1)
	7	16·66881	12·51685	−3·16678	1·22394(2)	−2·56808(2)	1·64451(1)	−2·65398(2)	1·64501(1)
	8	17·52218	13·66712	3·45360	−9·59495(3)	1·79660(2)	−1·45290(1)	1·86575(2)	−1·45660(1)
	9	18·35196	14·73678	−3·72164	7·73990(3)	−9·57606(3)	1·32364(1)	−1·01093(2)	1·32917(1)
	10	19·15580	15·73999	3·97368	−6·39337(3)	2·65909(3)	−1·20281(1)	3·06132(3)	−1·20919(1)
30	1	10·34553	1·90272	−1·01637	1·96972(1)	−3·16363(4)	1·43593	−3·13166(4)	1·15256
	2	16·11001	4·57067	1·38436	−8·23735(2)	9·70080(5)	−7·01989(1)	1·03470(4)	−6·56469(1)
	3	18·38887	6·98667	−1·70086	5·03248(2)	−4·62563(4)	4·53887(1)	−4·50251(4)	4·38279(1)
	4	19·83723	9·12393	2·02230	−3·44281(2)	2·22997(3)	−3·33199(1)	2·41994(3)	−3·26444(1)
	5	20·81964	11·02298	−2·34684	2·47819(2)	−6·79497(3)	2·65689(1)	−6·52126(3)	2·62491(1)
	6	21·53942	12·73226	2·66408	−1·84369(2)	1·00803(2)	−2·22321(1)	1·08523(2)	−2·20791(1)
	7	22·30933	14·29137	−2·96731	1·41045(3)	−7·22753(3)	1·93372(1)	−7·52394(3)	1·92705(1)
	8	23·15734	15·72988	3·25424	−1·10718(2)	1·30772(3)	−1·71235(1)	1·64345(3)	−1·71036(1)
	9	24·02714	17·06960	−3·52510	8·89962(3)	6·12010(3)	1·55451(1)	5·86619(3)	1·55525(1)
	10	24·89638	18·32688	3·78117	−7·30725(3)	−1·35149(2)	−1·41700(1)	−1·33345(2)	−1·41932(1)
45	1	14·16500	1·90798	−1·01523	1·96876(1)*	−6·94184(6)*	1·45679	−6·89111(6)*	1·17171
	2	22·02522	4·65096	1·36594	−8·26970(2)	4·87780(7)	−7·50233(1)*	5·14679(7)	−7·02608(1)*
	3	25·25138	7·26195	−1·63922	5·14538(2)	−1·41866(6)	5·07393(1)	−1·36730(6)	4·89890(1)
	4	27·39028	9·68721	1·90464	−3·62891(2)	2·37712(6)	−3·81266(1)	3·24393(6)	−3·72986(1)
	5	28·97818	11·92086	−2·17765	2·70520(2)	4·70337(5)	3·06852(1)	5·05210(5)	3·02473(1)
	6	30·20901	13·97869	2·45677	−2·07762(2)	−7·15556(4)	−2·57922(1)	−6·78293(4)	−2·55482(1)
	7	31·15930	15·88326	−2·73589	1·62809(2)	5·07048(3)	2·24916(1)	5·18345(3)	2·23540(1)
	8	31·87402	17·65669	3·00957	−1·29753(2)	−1·61588(2)	−1·99695(1)	−1·58925(2)	−1·98936(1)
	9	32·56308	19·31814	−3·27444	1·05066(2)	2·93285(2)	1·81613(1)	2·93821(2)	1·81232(1)
	10	33·35272	20·88341	3·52899	−8·64003(3)	−3·95280(2)	−1·65883(1)	−3·95108(2)	−1·65736(1)
∞	1		1·91227	−1·01430	1·96798(1)		1·47643		1·18997
	2		4·72278	1·34924	−8·29712(2)		−8·06124(1)		−7·56551(1)
	3		7·54721	−1·57231	5·25548(2)		5·88762(1)		5·69082(1)
	4		10·37402	1·74600	−3·84652(2)		−4·75850(1)		−4·65367(1)
	5		13·20159	−1·89085	3·03377(2)		4·05021(1)		3·98523(1)
	6		16·02951	2·01646	−2·50479(2)		−3·55757(1)		−3·51338(1)
	7		18·85760	−2·12815	2·13303(2)		3·19170(1)		3·15971(1)
	8		21·68580	2·22923	−1·85744(2)		−2·90737(1)		−2·88315(1)
	9		24·51407	−2·32190	1·64496(2)		2·67896(1)		2·65998(1)
	10		27·34239	2·40772	−1·47613(2)		−2·49066(1)		−2·47539(1)

* $X(a)$ means $X \times 10^{-a}$.

e.g.

$$\tilde{X}_1 = X_1(\eta)/\sqrt{\Delta_1}$$

$$\tilde{X}_2 = \begin{vmatrix} \int_0^1 X_1^2\,d\eta & X_1(\eta) \\ \int_0^1 X_2X_1\,d\eta & X_2(\eta) \end{vmatrix} \Big/ \sqrt{(\Delta_1\Delta_2)}$$

$$\vdots$$

$$\tilde{X}_n = \frac{\begin{vmatrix} \int_0^1 X_1^2\,d\eta & \int_0^1 X_1X_2\,d\eta & \cdots & \cdots & \int_0^1 X_1X_{n-1}\,d\eta & X_1(\eta) \\ \int_0^1 X_2X_1\,d\eta & \int_0^1 X_2^2\,d\eta & \cdots & \cdots & \int_0^1 X_2X_{n-1}\,d\eta & X_2(\eta) \\ \cdots & \cdots & \cdots & \cdots & \cdots & \cdots \\ \cdots & \cdots & \cdots & \cdots & \cdots & \cdots \\ \cdots & \cdots & \cdots & \cdots & \cdots & \cdots \\ \int_0^1 X_nX_1\,d\eta & \int_0^1 X_nX_2\,d\eta & \cdots & \cdots & \int_0^1 X_nX_{n-1}\,d\eta & X_n(\eta) \end{vmatrix}}{\sqrt{(\Delta_n\Delta_{n-1})}}$$

where Δ_n is the Gram-determinant which can be obtained by replacing the elements in the last column of the above determinant, $X_i(\eta)$, by $\int_0^1 X_iX_n\,d\eta$ ($i = 1, 2, \ldots, n$). In this study, $\tilde{X}_k$ and $\tilde{Y}_k$ are constructed for $k = 1$–20. Values of p_n^k and q_n^k can then be obtained for various Pe values. Just like X_n and Y_n, $\tilde{X}_n$ and $\tilde{Y}_n$ are independent of Q.

Substitution of equation (17) into (16) yields

$$\sum_{n=1}^{\infty}\sum_{k=n}^{\infty}(A_kp_n^k\tilde{X}_n - B_kq_n^k\tilde{Y}_n) = -1 + \frac{Q}{4}(1-\eta^2) \tag{19}$$

$$\sum_{n=1}^{\infty}\sum_{k=n}^{\infty}(\alpha_k^2A_kp_n^k\tilde{X}_n + \beta_k^2B_kq_n^k\tilde{Y}_n) = 0.$$

Multiplying the first equation by $\tilde{X}_m$, the second by $\tilde{Y}_m$, integrating with η from 0 to 1, and recalling the orthonormal properties of equation (18), the above coupled equations become

$$\sum_{k=m}^{\infty}A_kp_m^k - \sum_{n=1}^{\infty}\sum_{k=n}^{\infty}B_kq_n^k\int_0^1\tilde{X}_m\tilde{Y}_n\,d\eta = -\int_0^1\left[1 - \frac{Q}{4}(1-\eta^2)\right]\tilde{X}_m\,d\eta \tag{20}$$

$$\sum_{n=1}^{\infty}\sum_{k=n}^{\infty}\alpha_k^2A_kp_n^k\int_0^1\tilde{X}_n\tilde{Y}_m\,d\eta + \sum_{k=m}^{\infty}\beta_k^2B_kq_m^k = 0.$$

Or, in matrix form,

$$[F] = [E]^{-1}[G] \tag{21}$$

where

$$[F] = \begin{bmatrix} A_1 \\ A_2 \\ \cdot \\ \cdot \\ \cdot \\ A_m \\ B_1 \\ B_2 \\ \cdot \\ \cdot \\ \cdot \\ B_m \end{bmatrix} \qquad [G] = \begin{bmatrix} -\int_0^1 \left[1 - \frac{Q}{4}(1-\eta^2)\right] \tilde{X}_1 \mathrm{d}\eta \\ -\int_0^1 \left[1 - \frac{Q}{4}(1-\eta^2)\right] \tilde{X}_2 \mathrm{d}\eta \\ \cdot \\ \cdot \\ \cdot \\ \cdot \\ \cdot \\ -\int_0^1 \left[1 - \frac{Q}{4}(1-\eta^2)\right] \tilde{X}_m \mathrm{d}\eta \\ 0 \\ 0 \\ \cdot \\ \cdot \\ 0 \end{bmatrix}$$

$$[E] = \begin{bmatrix} p_1^1 & p_1^2 & \cdots & p_1^m & -q_1^1\int_0^1 \tilde{X}_1 \tilde{Y}_1 \mathrm{d}\eta & \cdots & -\sum_{k=1}^m q_k^m \int_0^1 \tilde{X}_1 \tilde{Y}_k \mathrm{d}\eta \\ 0 & p_2^2 & \cdots & p_2^m & & & \\ \cdot & \cdot & \cdots & \cdot & \cdot & \cdots & \cdot \\ \cdot & \cdot & \cdots & \cdot & \cdot & \cdots & \cdot \\ \cdot & \cdot & \cdots & \cdot & \cdot & \cdots & \cdot \\ 0 & 0 & \cdots & p_m^m & -q_1^1\int_0^1 \tilde{X}_m \tilde{Y}_1 \mathrm{d}\eta & \cdots & -\sum_{k=1}^m q_k^m \int_0^1 \tilde{X}_m \tilde{Y}_k \mathrm{d}\eta \\ \alpha_1^2 p_1^1 \int_0^1 \tilde{X}_1 \tilde{Y}_1 \mathrm{d}\eta & & \cdots & \alpha_m^2 \sum_{k=1}^m p_k^m \int_0^1 \tilde{X}_k \tilde{Y}_1 \mathrm{d}\eta & \beta_1^2 q_1^1 & \cdots & \beta_m^2 q_1^m \\ \alpha_1^2 p_1^1 \int_0^1 \tilde{X}_1 \tilde{Y}_2 \mathrm{d}\eta & & \cdots & \cdot & 0 & \cdots & \cdot \\ \cdot & & \cdots & \cdot & \cdot & \cdots & \cdot \\ \cdot & & \cdots & \cdot & \cdot & \cdots & \cdot \\ \cdot & & \cdots & \cdot & \cdot & \cdots & \cdot \\ \alpha_1^2 p_1^1 \int_0^1 \tilde{X}_1 \tilde{Y}_m \mathrm{d}\eta & & & \alpha_m^2 \sum_{k=1}^m p_k^m \int_0^1 \tilde{X}_k \tilde{Y}_m \mathrm{d}\eta & 0 & \cdots & \beta_m^2 q_m^m \end{bmatrix}$$

and $[E]^{-1}$ is the inverse matrix of $[E]$.

In this study, the infinite series appearing in equation (20) were truncated at $m = 20$. With $m = 20$, equation (21) yields forty simultaneous equations which were solved for the forty unknowns $A_1 \ldots A_{20}$ and $B_1 \ldots B_{20}$ by utilizing the Gauss elimination method with the aid of a CDC–6600 computer. The $[E]$ matrix was

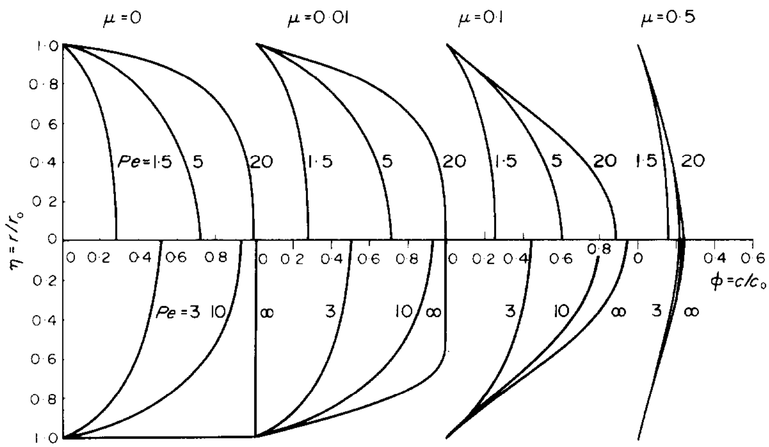

FIG. 1 (a). Concentration profiles in the $z > 0$ region of a tube. $Q = 0$.

normalized row-wise and reduced to a triangular form by transformations using pivotal condensations. The unknowns were then calculated by back substitutions. Whenever the computed series coefficients were found to be insufficiently accurate, a combination of Gauss elimination method and an iteration scheme was used to improve the computational accuracy. The first ten coefficients A_n and B_n thus obtained for $Pe = 1{\cdot}5, 3, 5, 10, 20, 30, 45, \infty$ and $Q = 0$ and $1{\cdot}0$ are tabulated in Table 1.

Having determined the coefficients A_n and B_n, the eigenvalues α_n and β_n, and the eigenfunctions $X_n(\eta)$ and $Y_n(\eta)$, $n = 1$–20, the local concentrations in the infinite region can then be found from equations (10) and (11). Of particular interest are the flow characteristics in the tube, $\mu > 0$ region. Some concentration profiles in that region for $Pe = 1{\cdot}5, 3, 5, 10, 20$ and ∞ are shown in Fig. 1(a, b) for two cases of diffusion, with and without generation in the tube. The concentrations for the generation case with $Q = 1$ are always, except at the tube walls and near the tube entrance for $Pe > 100$, higher than the case without generation ($Q = 0$), the differences being greater at smaller Péclét numbers.

The local dimensionless bulk concentration and the local Sherwood number in the tube ($\mu > 0$ region) can be readily found to be

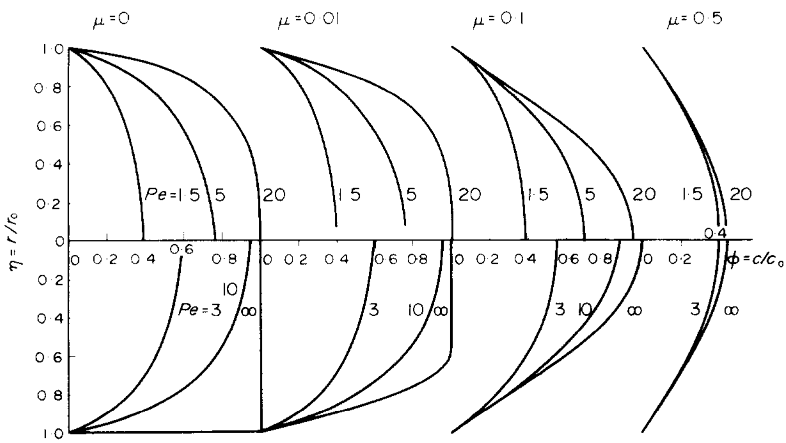

FIG. 1 (b). Concentration profiles in the $z > 0$ region of a tube, $Q = 1$.

$$\phi_b(\mu) = \frac{c_b}{c_0} = \frac{Q}{6} - 2\sum_{n=1}^{\infty} B_n \left\{ \frac{Y_n'(1)}{\beta_n^2} + \left(\frac{2}{Pe}\right)^2 \beta_n^2 \int_0^1 \eta Y_n(\eta)\,d\eta \right\} \exp(-\beta_n^2\mu) \quad (22)$$

and

$$Sh(\mu) = -\frac{2}{\phi_b}\left(\frac{\partial \phi_2}{\partial \eta}\right)_{\eta=1} = \frac{Q - \sum_{n=1}^{\infty} B_n Y_n'(1)\exp(-\beta_n^2\mu)}{\frac{Q}{6} - \sum_{n=1}^{\infty} B_n\left\{\frac{Y_n'(1)}{\beta_n^2} + \left(\frac{2}{Pe}\right)^2 \beta_n^2 \int_0^1 \eta Y_n(\eta) d\eta\right\}\exp(-\beta_n^2\mu)}. \quad (23)$$

As defined, $\phi_b(\mu)$ is the fraction of diffusing matters remaining in the fluid at a distance x from the tube entrance; and $Sh(\mu)$ physically depicts the rate of deposition of the diffusing matters at the tube walls.

In defining $\phi_b(\mu)$, the local axial particle flux has been taken to be the convective flux given by uc_2. To account for the additional axial diffusive flux, however, we may introduce another parameter $F^*(\mu)$ which can be shown to be

$$F^*(\mu) \equiv \frac{\int_0^{r_0}\left(uc_2 - D\frac{\partial c_2}{\partial x}\right)2\pi r dr}{\pi r_0^2 c_0 \bar{u}} = \frac{Q}{6} - 2\sum_{n=1}^{\infty} B_n \left\{\frac{Y_n'(1)}{\beta_n^2}\right\}\exp(-\beta_n^2\mu). \quad (24)$$

DISCUSSION AND CONCLUSIONS

One of the most crucial parts of this analysis is, undoubtedly, in the matching of the concentrations and the longitudinal concentration gradients at $\mu = 0$ to obtain the series expansion coefficients, A_n and B_n. The task is further complicated by the fact that, at small Péclét numbers, the consecutive higher eigenvalues do not vary appreciably in magnitude necessitating, therefore, a larger number of terms, equivalent to a larger number of higher eigenvalues, to be included in the summation in equation (21).

To ascertain that the series expansion coefficients, A_n and B_n, computed by constructing the orthonormal functions and by solving the system of forty simultaneous equations (with $m = 20$) indeed satisfy the required matching conditions, they were substituted into the left side of equation (16). The results were checked with the right side of these equations, and it was revealed that these two equations were both satisfied remarkably well for the Péclét numbers considered.* This proves the validity of the present solutions.

By employing the first twenty eigenvalues and the associated constants, the local dimensionless bulk concentrations were calculated from equation (22) for various values of Pe and Q. The bulk concentrations thus obtained are shown in Fig. 2 for $Pe = 1{\cdot}5$, 3, 5, 10, ∞ and $Q = 0$, $1{\cdot}0$. It is observed that as $\mu \to \infty$, $\phi_b \to Q/6$ for all Q's, as can also be seen from equation (22). This asymptotic trend is consistent with that found in the semi-infinite region analysis [2, 3, 8]. For finite values of μ, however, especially for $0 \leqslant \mu < 1$, $\phi_b(\mu)$ decreases rapidly with decreasing Péclét numbers throughout the entrance region. The bulk concentration curves for various Péclét numbers cross one another near $\mu \simeq 1$, reversing therefore the aforementioned trend before finally reaching the asymptotic value of $Q/6$ at $\mu \simeq 5$ for all Péclét numbers. The drastic decrease in bulk concentrations with decreasing Péclét numbers in the entrance region is apparently due to "back" diffusion at the tube inlet into the $\mu < 0$ region. The semi-

* Computations were also made with $m = 20$ for $Pe = 1{\cdot}0$, but the results are not too satisfactory due to slow convergence of the infinite series solution and hence are not included herein.

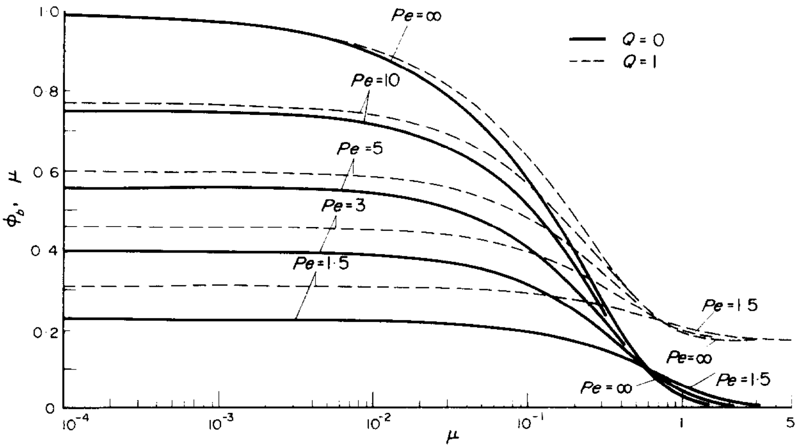

FIG. 2. Variations of local bulk concentration in $z > 0$ region, $Q = 0$ and 1.

infinite region analysis [3,8] assuming, *a priori*, a uniform concentration at $\mu = 0$ and thus providing no possibility of back diffusion at $\mu = 0$ into the $\mu < 0$ region, has predicted an increase in $\phi_b(\mu)$ with decreasing Péclét numbers.

The local Sherwood number, obtained from equation (23), is shown in Fig. 3 also for $Pe =$ 1·5, 3, 5, 10, ∞ and $Q = 0$, 1·0. The variations of $Sh(\mu)$ with Pe and Q are generally analogous to those obtained by the semi-infinite region analysis [3, 8], but the magnitude of $Sh(\mu)$ is appreciably reduced in the present infinite region analysis, again due to a decrease in concentration gradient at the tube walls in the presence of back diffusion. For non-zero values of Q, $Sh \to 6$ as $\mu \to \infty$, a trend which has been found in [2]. For $Q = 0$, however, the fully developed Sherwood numbers decrease slightly

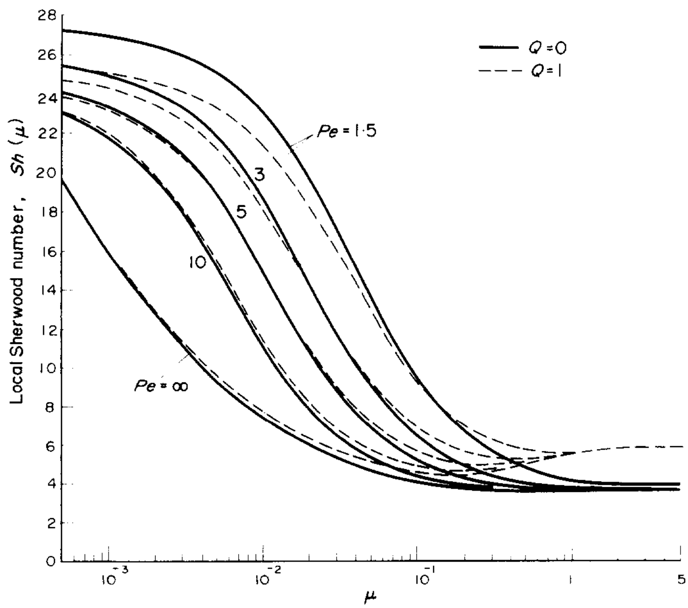

FIG. 3. Variations of local Sherwood number in $z > 0$ region, $Q = 0$ and 1.

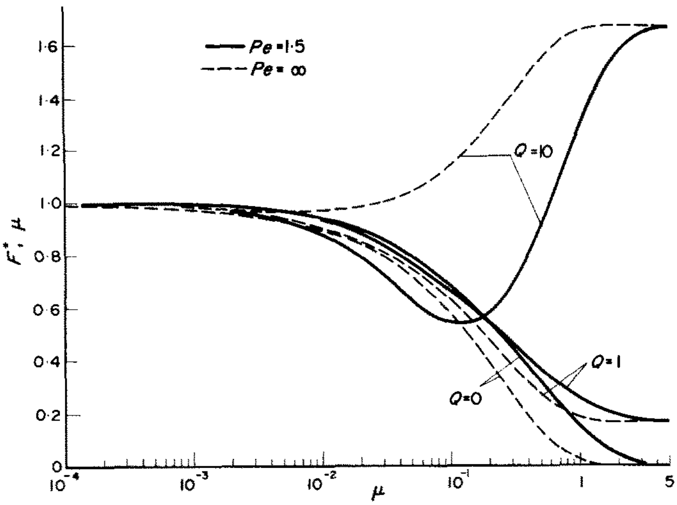

FIG. 4. Variations of $F^*(\mu)$ in $z > 0$ region, $Pe = 1{\cdot}5, \infty$ and $Q = 0, 1, 10$.

with increasing Péclét numbers as shown in the following:

	$Pe =$ 1·0	$Pe =$ 1·5	$Pe = 3$	$Pe = 5$	$Pe =$ 10	$Pe =$ 20
This study		3·9698	3·8507	3·7672	3·6951	3·6675
Tan [8]	4·0273			3·7672	3·6951	3·6675
Schmidt [4]	3·93				3·67	
Labuntsov [9]	4·04				3·74	

	$Pe =$ 30	$Pe =$ 45	$Pe =$ 50	$Pe =$ 100	$Pe =$ ∞
This study	3·6616	3·6589			3·6567
Tan [8]	3·6616		3·6585	3·6572	3·6567

It is observed, as it should be, that the fully developed Sherwood numbers for various Péclét numbers obtained in this analysis of diffusion in the infinite region $-\infty < z < +\infty$ are identical to the corresponding values derived from the semi-infinite region analysis [8]. Further, the values agree favorably with, and fall in between those values of Schmidt and Zeldin [4] and Labuntsov [9].

The variations of F^* with μ for $Pe = 1{\cdot}5$, ∞ and $Q = 0$, 1, 10 are shown in Fig. 4. It is seen that $F^* \to 1$ as $\mu \to 0$, while $F^* \to Q/6$ as $\mu \to \infty$ for all Pe and Q. As expected, the asymptotic trend of F^* is the same as that of ϕ_b as $\mu \to \infty$. It is interesting to note that, in the case with generation in the tube, $F^*(\mu)$ as well as $\phi_b(\mu)$ can become larger than unity far downstream from the tube inlet. This is the case when $Q > 6$ as can be seen from equations (22) and (24). Apparently at $Q > 6$, the generation rate far exceeds the loss of particles to the tube walls.

The results of this analysis, taking into consideration diffusion in the infinite region $-\infty < z + \infty$ deviate and, at times, are quite different from those based on the semi-infinite region $(0 < z < +\infty)$ analysis, especially in the tube entrance region. This is due to the different concentration profiles based on the two analyses. In the semi-infinite règion analysis, the concentration is uniform at $z = 0$; while in the infinite region analysis, the concentrations are far from uniform at $z = 0$ (Fig. 1) for finite values of Pe. In fact, back diffusion plays an important role if the Péclét number is small; and it is incorrect to assume a uniform concentration profile at $z = 0$ when the effect of axial diffusion is significant at small Péclét numbers. Instead, the concentration profile should be taken to be uniform at $z = -\infty$ in analyzing the effect of axial diffusion in channel flow, as is done in the present analysis.

REFERENCES

1. C. J. Hsu, An exact mathematical solution for entrance-region laminar heat transfer with axial conduction, *Appl. Sci. Res.* **17**, 359–376 (1967).
2. C. W. Tan and C. J. Hsu, Mass transfer of decaying products with axial diffusion in cylindrical tubes, *Int. J. Heat Mass Transfer* **13**, 1887–1905 (1970).
3. C. W. Tan and C. J. Hsu, Diffusion of aerosols in laminar flow in a cylindrical tube, *Aerosol Sci.* **2**, 117–124 (1971).
4. F. W. Schmidt and B. Zeldin, Laminar heat transfer in the entrance region of ducts, *Appl. Sci. Res.* **23**, 73–94 (1970).
5. C. J. Hsu, An exact analysis of low Péclét number thermal-entry-region heat transfer in transversely non-uniform velocity fields, To be published in *A.I.Ch.E. Journal*.
6. C. J. Hsu, Theoretical solutions for low-Péclét-number thermal-entry-region heat transfer in laminar flow through concentric annuli, *Int. J. Heat Mass Transfer* **13**, 1907–1924 (1970).
7. C. W. Tan, Diffusion of disintegration products of inert gases in cylindrical tubes, *Int. J. Heat Mass Transfer* **12**, 471–478 (1969).
8. C. W. Tan, Mass transfer of aerosols with axial diffusion in circular tubes, U.S. Atomic Energy Commission, Health and Safety Laboratory Report HASL-238 (Oct. 1970).
9. D. A. Labuntsov, Heat emission in pipes during laminar flow of a liquid with axial heat conduction taken into account, *Sov. Phys. Dockl.* **3**, 33 (1958).

TRANSFERT MASSIQUE A FAIBLE NOMBRE DE PECLET DANS UN ECOULEMENT LAMINAIRE A L'INTERIEUR DE TUBES CIRCULAIRES

Résumé—On étudie le transfert massique dans la région d'entrée de matières qui diffusent dans l'écoulement laminaire à l'intérieur d'un tube circulaire dans deux cas de diffusion avec ou sans formation de particules dans le tube. Pour tenir compte des effets de la diffusion axiale sensible à de faibles nombres de Péclét de diffusion *Pe*, le domaine de diffusion est étendu à la région en amont du tube ($z < 0$) ainsi qu'à celle correspondant au tube ($z < 0$) et une concentration uniforme est admise à $z = -\infty$. Les valeurs propres sont calculées pour les deux régions et les vingt premières sont obtenues pour Pe = 1,5; 3; 5; 10; 20; 30; 45 et ∞. En établissant deux systèmes de fonctions orthonormées à partir des fonctions propres non orthogonales, les coefficients de développement en série sont alors déterminés en raccordant à $z = 0$ les concentrations et les gradients de concentration longitudinaux des deux régions. Les solutions de la concentration correspondant à $Pe = \infty$ sont en excellent accord avec notre précédente analyse de la région semi-infinie ($z > 0$). Les effets de la diffusion axiale sur les distributions de concentration, les fractions des espèces diffusantes qui pénètrent dans le tube et le nombre de Sherwood local sont présentés pour différents nombres de Péclét et pour un paramètre de génération de particule Q.

STOFFAUSTAUSCH BEI LAMINARER STRÖMUNG MIT KLEINEN PECLET-ZAHLEN IN ROHREN MIT KREISQUERSCHNITT

Zusammenfassung—Für laminare Strömung in einem Rohr mit Kreisquerschnitt wird die Stoffübertragung diffundierender Stoffe im Eintrittsbereich untersucht, wobei zwei Arten von Diffusion betrachtet werden: mit und ohne Teilchenbildung während des Strömungsvorgangs. Um die Effekte der Diffusion in axialer Richtung zu berücksichtigen, die bei niedrigen Diffusions-Péclét-Zahlen wichtig werden, wird der Bereich der Diffusion auf den Bereich vor dem Rohr ($z < 0$), über den im Rohr ($z > 0$) hinaus ausgedehnt. Gleichförmige Konzentration erhält man bei $z = -\infty$. Die Eigenwerte werden für die zwei Bereiche berechnet, wobei man die ersten zwanzig für Pe = 1·5, 3,5, 10, 20, 30, 45 und ∞ erhält. Wenn man aus den nicht-orthogonalen Eigenfunktionen zwei Sätze von orthonormalen Funktionen konstruiert, kann man die Koeffizienten der Reihenentwicklung bestimmen, indem man die Konzentration und den Konzentrationsgradienten in axialer Richtung für beide Bereiche an der Stelle $x = 0$ gleichsetzt. Die Lösungen für die Konzentration, entsprechend $Pe = \infty$, stimmen hervorragend mit unserer früheren Analyse im halbunendlichen Bereich ($z > 0$) überein. Die Auswirkungen der Diffusion in axialer Richtung auf die Konzentrationsverteilungen, der Anteil der diffundierenden Stoffe, die das Rohr durchdringen, und die lokale Sherwood-Zahl werden für verschiedene Péclét-Zahlen und für einen Parameter Q angegeben, der die Teilchenbildung beschreibt.

МАССООБМЕН ПРИ ЛАМИНАРНОМ ТЕЧЕНИИ В КРУГЛЫХ ТРУБАХ ПРИ МАЛЫХ ЗНАЧЕНИЯХ ЧИСЛА ПЕКЛЕ

Аннотация—Проведено исследование массообмена диффундирующих частиц во входном круглой трубы при ламинарном течении для двух случаев диффузии: при наличии такого образования частиц во время движения в трубе и при его отсутствии. Для учета влияния диффузии вдоль оси движения, существенной при малых диффузионных

числах Пекле, область диффузии была расширена за пределы трубы ($z < 0$), включая участок выше трубы ($z > 0$), и на $z = -\infty$ задавался равномерный профиль концентрации. Собственные значения рассчитывались для двух областей, и первые двадцать значений получены для $Pe = 1{,}5$; 3; 5; 10; 20; 30; 45; и ∞. Построены две системы ортонормальных функций по двум неортонормальным собственным функциям, а затем определены коэффициенты разложения в ряд методом подбора пары значений концентрации и градиентов продольной концентрации для двух областей при $z = 0$. Решения для концентраций, соответствующих $Pe = \infty$, находятся в хорошем соответствии с проведенным ранее анализом для полубесконечной области ($z > 0$). Представлены зависимости распределения концентрации, относительной концентрации диффундирующих материалов, проникающих в трубу, и локального числа Шервуда от диффузии вдоль оси для различных чисел Пекле и параметра образования частиц Q.